Review Article | Neuroimaging and Head & Neck

http://dx.doi.org/10.3348/kjr.2015.16.4.749
pISSN 1229-6929 · eISSN 2005-8330
Korean J Radiol 2015;16(4):749-766

Korean Journal of Radiology
KJR

Ultrasonography-Based Thyroidal and Perithyroidal Anatomy and Its Clinical Significance

Eun Ju Ha, MD[1], Jung Hwan Baek, MD, PhD[2], Jeong Hyun Lee, MD, PhD[2]

[1]Department of Radiology, Ajou University School of Medicine, Suwon 443-380, Korea; [2]Department of Radiology and Research Institute of Radiology, University of Ulsan College of Medicine, Asan Medical Center, Seoul 138-736, Korea

Ultrasonography (US)-guided procedures such as ethanol ablation, radiofrequency ablation, laser ablation, selective nerve block, and core needle biopsy have been widely applied in the diagnosis and management of thyroid and neck lesions. For a safe and effective US-guided procedure, knowledge of neck anatomy, particularly that of the nerves, vessels, and other critical structures, is essential. However, most previous reports evaluated neck anatomy based on cadavers, computed tomography, or magnetic resonance imaging rather than US. Therefore, the aim of this article was to elucidate US-based thyroidal and perithyroidal anatomy, as well as its clinical significance in the use of prevention techniques for complications during the US-guided procedures. Knowledge of these areas may be helpful for maximizing the efficacy and minimizing the complications of US-guided procedures for the thyroid and other neck lesions.

Index terms: *Thyroid; Ultrasonography; RF ablation; Nerve block; Core needle biopsy*

INTRODUCTION

Recently, ultrasonography (US)-guided minimally invasive procedures such as ethanol ablation, radiofrequency (RF) ablation, and laser ablation, as well as selective nerve block, have been introduced with good results (1-4). US-guided core-needle biopsy (CNB) has also been widely applied in the diagnosis of thyroid nodules and neck tumors, including lymph nodes, to replace conventional fine-needle aspiration (FNA) (5-12). These procedures manage thyroid and neck lesions effectively and prevent unnecessary surgery, hence, they are being incorporated in standard management of thyroid and neck lesions (5-7, 9-11).

However, various procedure-related complications due to the injuries of small neurovascular structures have been reported (13-15). The establishment of US-based anatomy, rather than cadaver-based, CT-based, or MRI-based anatomy, is necessary to maximize the efficacy and minimize the complications of US-guided procedures of the neck. However, few articles have focused on the features of US and their clinical significance from a preventive aspect of complications (16, 17). Therefore, the purposes of this educational review were to: 1) systematically describe US-based thyroidal and perithyroidal anatomy; 2) to explain its clinical significance; and 3) to provide prevention techniques for complications during US-guided procedures.

Nervous System

Among the anatomic structures, nerve injuries may be serious complications in practice, and are therefore

Received November 4, 2014; accepted after revision May 13, 2015.
Corresponding author: Jung Hwan Baek, MD, PhD, Department of Radiology and Research Institute of Radiology, University of Ulsan College of Medicine, Asan Medical Center, 88 Olympic-ro 43-gil, Songpa-gu, Seoul 138-736, Korea.
• Tel: (822) 3010-4348 • Fax: (822) 476-0090
• E-mail: radbaek@naver.com

discussed in detail (Fig. 1). Normal peripheral nerves can usually be demonstrated with high-resolution US; however, the US feature of the nerve may vary depending on the equipment used, location in the neck, and size of the nerve (18-20). With 10–17 MHz frequency probes, the nerve is seen as a honeycomb or reticular pattern with approximately 2 to 8 hypoechoic rounded fascicles according to size surrounded by hyperechoic epineurium (18-21). On longitudinal scans, the nerve is seen as a striated pattern with several parallel echogenic lines of its internal structures (Fig. 2). Detection of small nerves may be operator-dependent, and requires a longer learning curve due to difficulties in identifying subtle anatomic details using US.

The knowledge of nerve location and variation is important in differentiating a neurogenic tumor from a metastatic lymph node and in preventing nerve injuries during US-guided procedures (22-24). Intra-procedural nerve injury results in various symptoms ranging from purely transient to permanent that depend on the severity and duration of the injury (13). We described in detail the US features, relationship with other structures, and injury symptoms for each nerve in the neck involved in US-guided procedures.

Vagus Nerve

The vagus nerve is the longest cranial nerve. The cervical course of the vagus nerve can be easily visualized on US as a 2-mm to 3-mm diameter structure. It is typically located within the carotid sheath, and is usually posterolateral to the common carotid artery (CCA) and posteromedial to the internal jugular vein (IJV) (20, 21). The variation in the cervical course of the vagus nerve according to its position relative to the CCA has been previously reported (23, 25). The anterior variation in which the nerve passes in front of the CCA, is relatively common with a reported prevalence of up to 18.9%; whereas, medial or posterior variation has a lower prevalence (Fig. 3). A bulging thyroid mass outside the thyroid gland could also change the vagus nerve location anterior to the CCA by pushing the carotid sheath laterally and inducing vagus nerve variation (Fig. 4) (23).

Vagal schwannoma could be easily misdiagnosed as a metastatic lymph node causing unnecessary FNAs or diagnostic surgery (22). However, a typical location within the carotid sheath and direct continuity with the vagus nerve are characteristic US features of vagal schwannoma (26). For minimally invasive treatment such as RF ablation of thyroid nodules, attention to the vagus nerve location relative to the thyroid nodule is necessary to prevent nerve injuries. The variation in the vagus nerve location could increase the proximity of the vagus nerve to the thyroid gland, increasing its vulnerability to thermal injury (Figs. 3, 4). Therefore, operators should be aware of possible injuries to the vagus nerve located near the lateral margin of the benign thyroid nodules and also at the lateral neck during the treatment of recurrent thyroid cancers (13, 23).

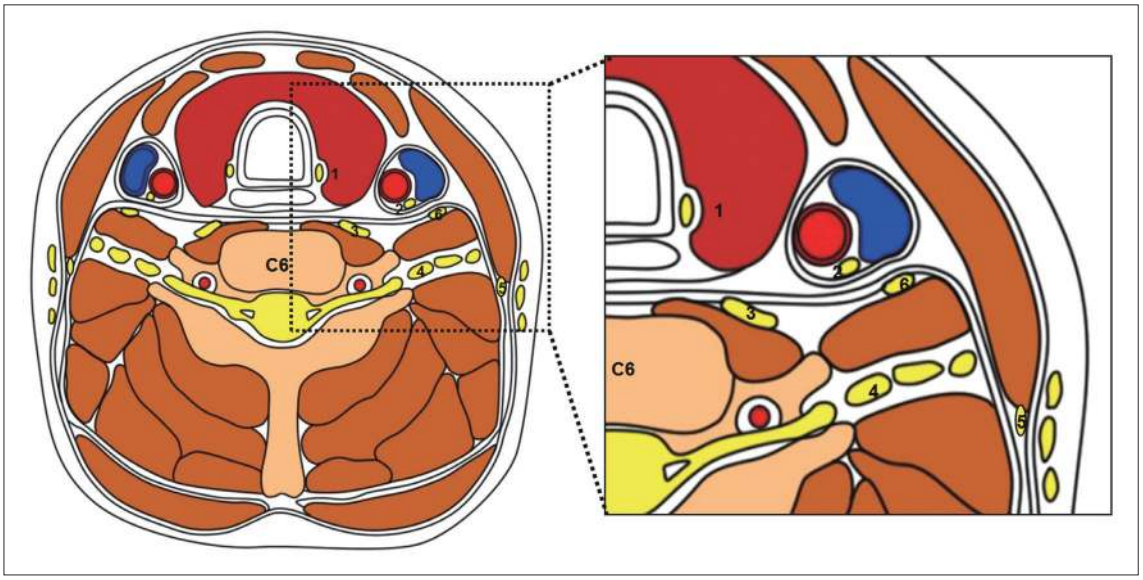

Fig. 1. Schematic drawing of transverse section of neck at C6 level. Relationship of neck nerves to adjacent anatomic structures is shown. 1 = recurrent laryngeal nerve, 2 = vagus nerve, 3 = cervical sympathetic ganglion, 4 = cervical/brachial plexus, 5 = spinal accessory nerve, 6 = phrenic nerve

Korean Journal of Radiology
KJR

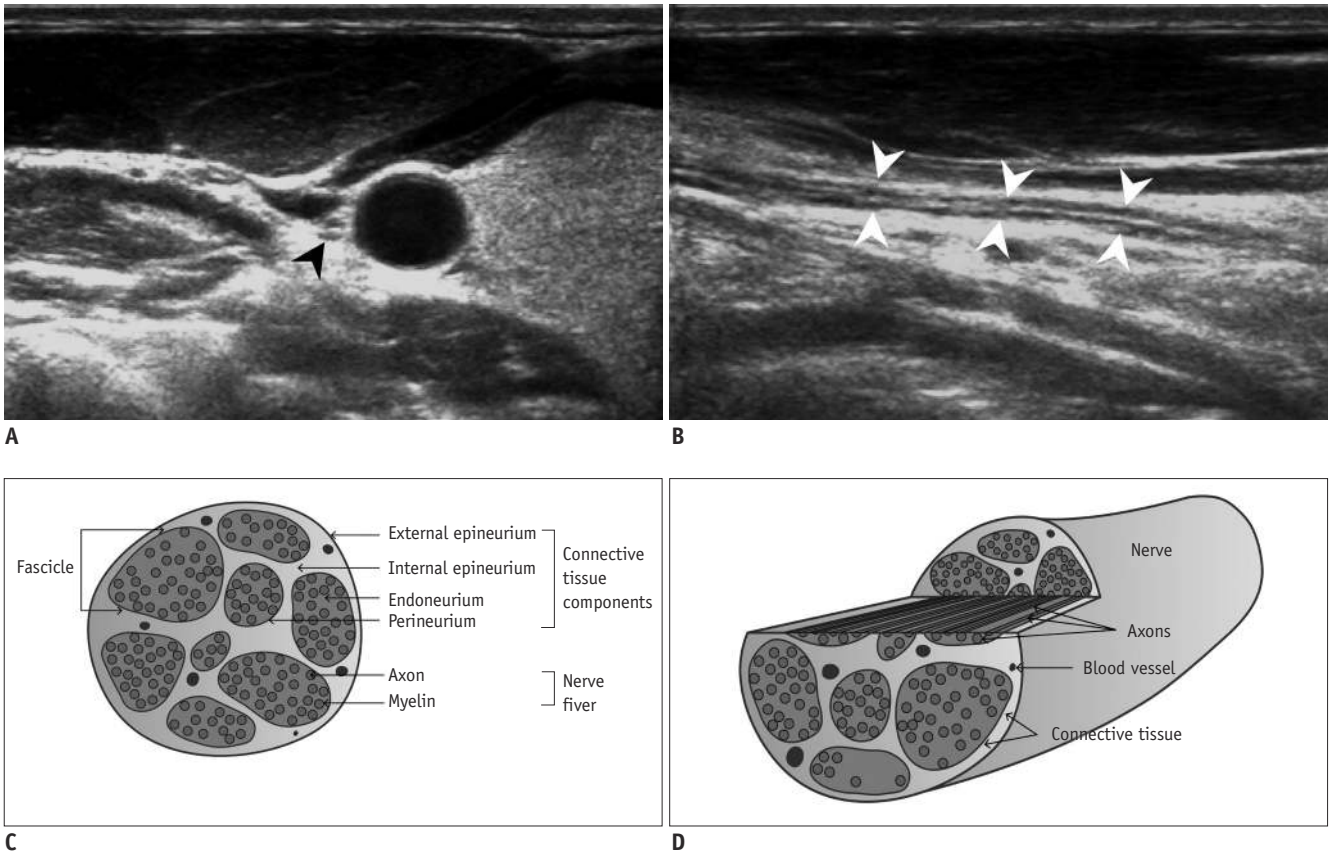

Fig. 2. Ultrasonography (US) features and histologic correlation of neck nerve.
A. On transverse scan, nerve (arrowhead) is seen as honeycomb or reticular pattern with small, hypoechoic, rounded structures. **B.** On longitudinal scan, it is seen as striated pattern with several parallel echogenic lines (arrowheads). **C, D.** Schematic histologic structure of nerve bundle corresponds to US features.

Various symptoms could develop after vagus nerve injury. Because the cervical portion of the vagus nerve is cranial to the origin of the recurrent laryngeal nerve (RLN), vagus nerve injury may cause symptoms as a result of dysfunction of the RLN (e.g., cough, voice change) or dysfunction of the vagus nerve itself (e.g., arrhythmia, dysphagia, dyspnea, nausea, hiccups) (20). The latter symptoms are not specific to vagus nerve injury; therefore, significant diagnostic delays may occur, and patients may undergo unnecessary examinations.

Superior and Inferior Laryngeal Nerves

Recurrent and Non-Recurrent Inferior Laryngeal Nerve

The RLN is a branch of the vagus nerve that supplies the intrinsic muscles of the larynx. The RLN is not directly visualized on US due to its small diameter. Therefore, knowledge of its expected course and variation is essential to prevent complications during the procedures (Fig. 5). The right and left RLNs are not symmetrical in course, with the left nerve looping under the aortic arch and the right nerve traveling directly upwards after curving below the subclavian artery. At the level of the neck, they are located in the tracheoesophageal groove, passing posteromedially to both lobes of the thyroid. They then penetrate the larynx posterior to the cricoarytenoid joints at the level of the thyroid cartilage.

A variation in the RLN is called the non-recurrent laryngeal nerve (NRLN), which passes from the vagus nerve directly into the larynx at the level of the inferior horn of the thyroid cartilage. It reportedly occurs in 0.5–0.6% cases on the right side and 0.004% on the left side (27-30). Because the right NRLN is associated with the aberrant right subclavian artery arising directly from the aortic arch, and the left NRLN is associated with the situs inversus, anatomical variation could be suspected when a vascular anomaly is identified by CT or MRI (31). US can also predict the NRLN with identification of the absence of the brachiocephalic trunk (Fig. 6) (32, 33). The division of the brachiocephalic artery into the CCA and subclavian artery

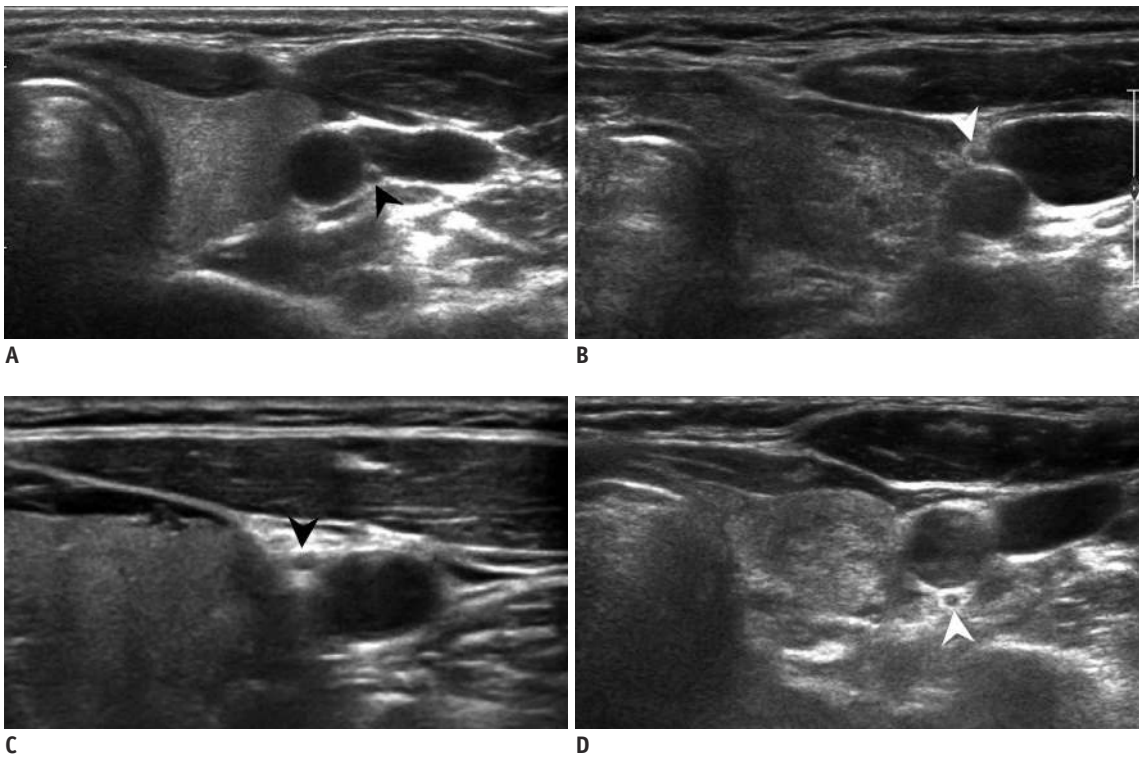

Fig. 3. Transverse ultrasonography images of vagus nerve.
(A) Vagus nerve (arrowhead) is usually located posterolateral to common carotid artery. However, vagus nerve (arrowheads) can be located anterior **(B)**, medial **(C)**, and posterior **(D)** to common carotid artery, and these variations place it closer to thyroid gland.

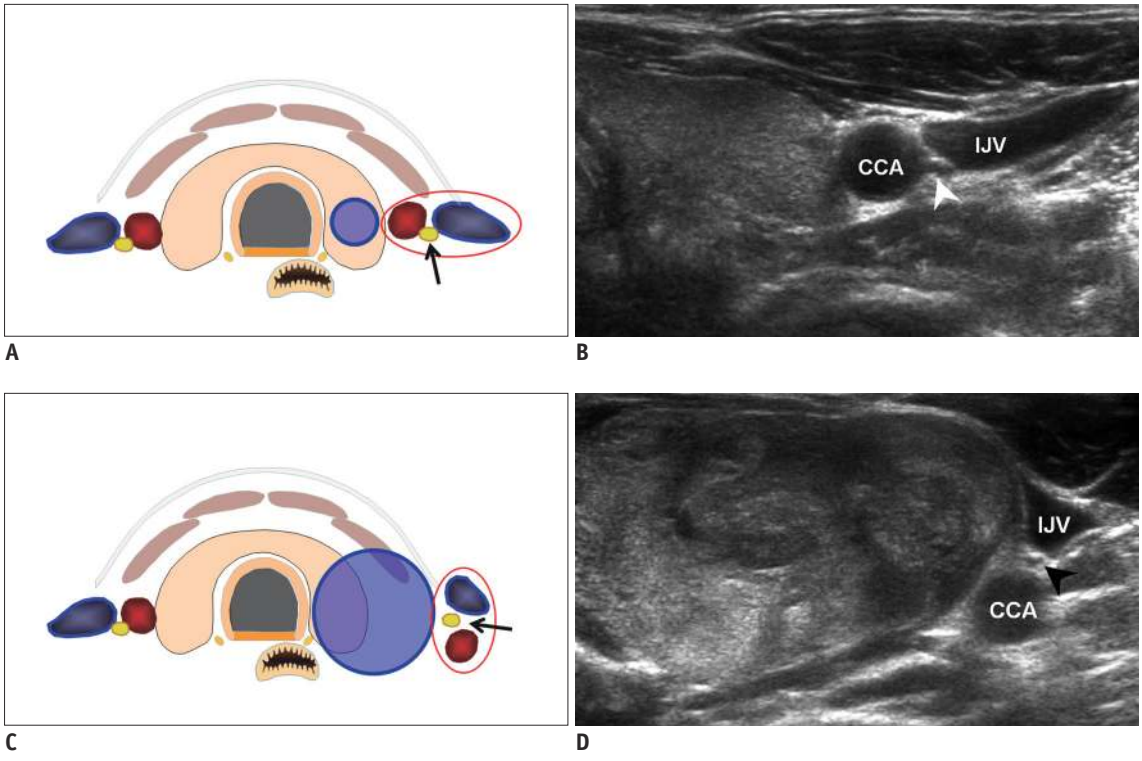

Fig. 4. Change of vagus nerve location by bulging thyroid mass.
A, B. In normal thyroid gland, CCA, vagus nerve (yellow circle, arrowhead), and IJV are located in horizontal direction. **C, D.** In patients with bulging thyroid mass, their positions are changed to vertical direction and vagus nerve (yellow circle, arrowhead) is located anterior to CCA. CCA = common carotid artery, IJV = internal jugular vein

Korean Journal of Radiology
KJR

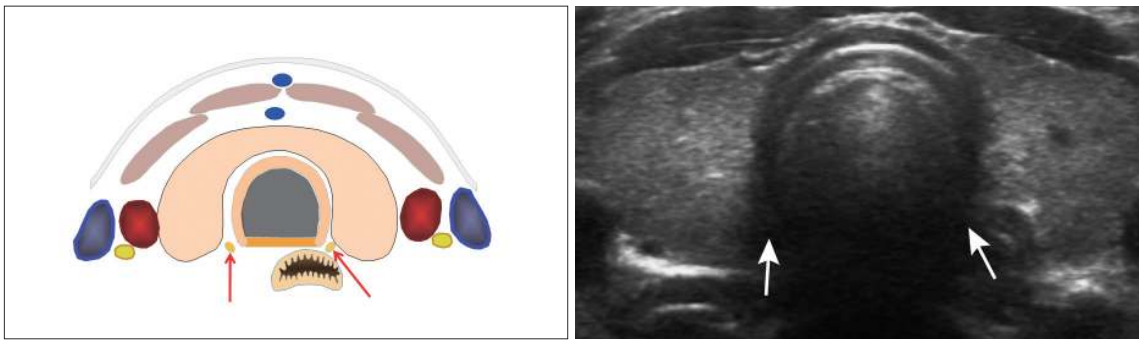

A B

Fig. 5. Relationship of recurrent laryngeal nerves to adjacent anatomic structures.
A. Schematic drawing shows location of recurrent laryngeal nerve (arrows). **B.** Although recurrent laryngeal nerve is not directly visualized on ultrasonography, its location can be expected in tracheoesophageal groove (arrows).

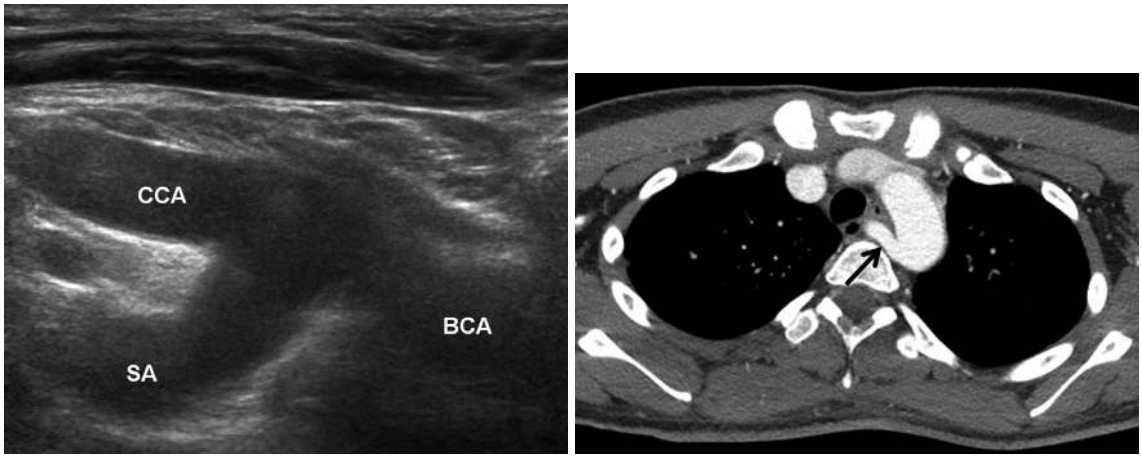

A B

Fig. 6. Normal and absence of brachiocephalic artery.
A. Normal division of BCA into CCA and SA is called Y sign. **B.** In patients with non-recurrent laryngeal nerve, right aberrant SA (arrow) arises directly from aortic arch. BCA = brachiocephalic artery, CCA = common carotid artery, SA = subclavian artery

has been described as the Y sign. Hence, operators should look for the Y sign to rule out the possibility of an NRLN.

Recurrent laryngeal nerve injury causes symptoms such as voice change and cough, and is usually caused by an injury during biopsy or minimally invasive treatment. FNA or CNB for thyroid or neck lesions can cause direct damage by needle or compression by swelling or hematoma (34). Direct thermal or chemical injury to the RLN can occur during minimally invasive treatment (13, 35). Minimizing heat exposure to the tracheoesophageal groove (so called as a danger triangle which includes the RLN, trachea, and esophagus) is crucial to prevent complications; thus, operators should be aware of possible injuries to the RLN located near the posteromedial portion of the thyroid gland and also for the treatment of recurrent tumors at the operation bed (13, 35, 36). The small remnant of thyroid tissue could be detected after thyroid surgery near the lateral thyrohyoid ligament (ligament of Berry) to prevent RLN injury during surgery (37). Understanding these anatomies could prevent unnecessary FNAs or diagnostic surgery for remnant thyroid tissue (Fig. 7).

Superior Laryngeal Nerve

The superior laryngeal nerve (SLN) is a branch of the vagus nerve that is separated high in the neck. It descends in the neck adjacent to the pharynx, medial to the carotid sheath, and divides into the internal and external branches approximately 2–3 cm superior to the thyroid gland. It then enters the vocal cord through the cricothyroid membrane (Fig. 8). The external branch supplies the cricothyroid muscles, and injury to the nerve changes the pitch of the voice and causes an inability to make explosive sounds. Although it is not visible on US, its location could be expected near the superior thyroidal artery and vein at the superior aspect of the thyroid gland. Therefore, attention to SLN injury is necessary when treating recurrent tumors

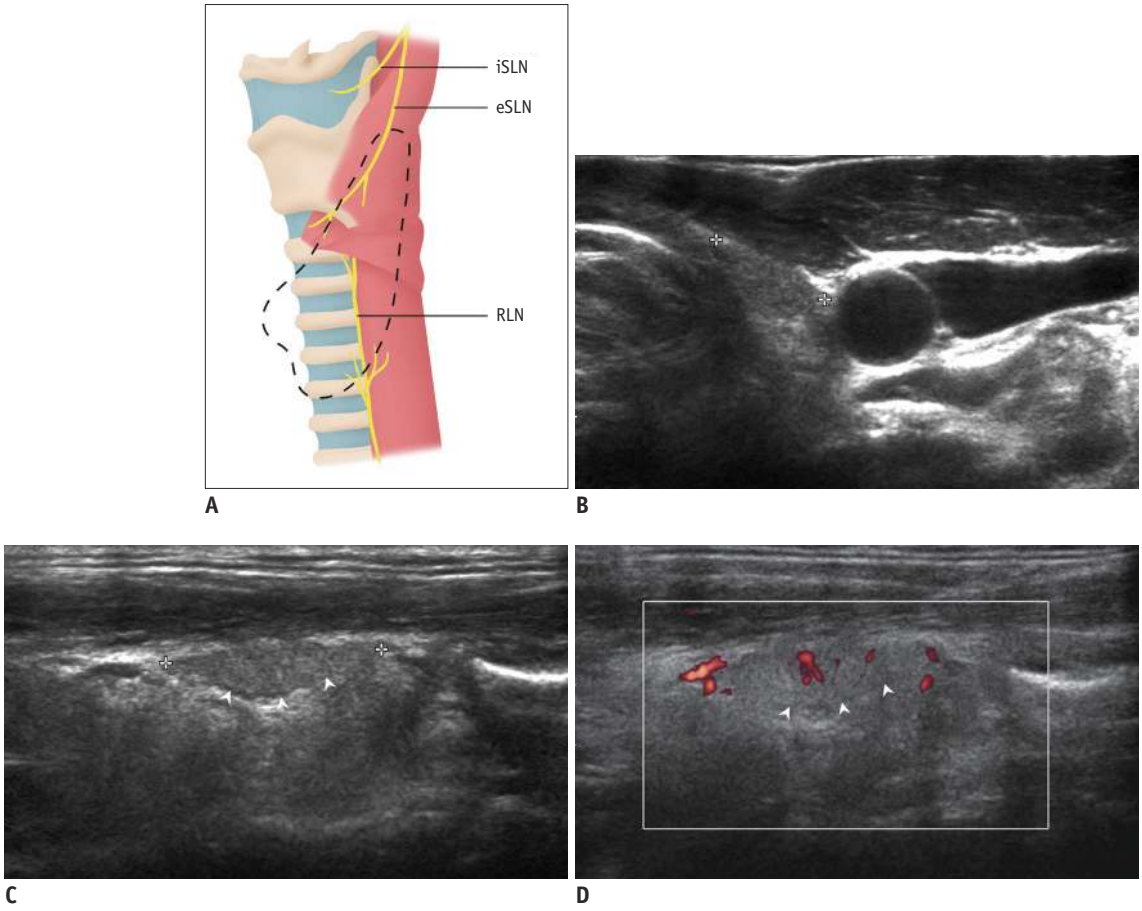

Fig. 7. Small remnant of thyroid tissue.
A. Schematic drawing shows RLN course at ligament of Berry. Dotted line represents thyroid gland. **(B)** On transverse and **(C, D)** longitudinal scans, small remnant of thyroid tissue (arrowheads) can be seen at upper pole of thyroid gland after thyroid surgery. eSLN = external branch of superior laryngeal nerve, iSLN = internal branch of superior laryngeal nerve, RLN = recurrent laryngeal nerve

medial to the superior thyroidal artery at the upper pole of the thyroid gland during RF ablation (Fig. 8). The internal branch dominates sensory sensation above the vocal cord, and is located between the greater horn of the hyoid bone and thyroid cartilage just above the thyrohyoid membrane. SLN block may be performed using these anatomic landmarks (38).

Cervical Sympathetic Ganglion

The cervical sympathetic ganglion (CSG) consists of 3 paravertebral ganglia. The superior CSG is the largest, and is located anterior to the longus capitis muscle at the C2–3 vertebra level; the middle CSG is the smallest, and is located anterior to the longus colli muscle at the C5–7 vertebra level; the inferior CSG is intermediate in size, and is commonly fused with the first thoracic ganglion to form a stellate ganglion at the C7–T1 vertebra level (39). Because the middle CSG is located at the lower level of the thyroid gland, it can be injured during procedures for thyroid lesions. The middle CSG can be visualized in 41% of US images, and is seen as a spindle-shaped hypoechoic structure with a mean diameter of 3.8 ± 1.5 mm and a length of 8.7 ± 3.2 mm on US (40). It is usually located lateral to the CCA, but can also be located medial to the CCA (Fig. 9) (40). Because the middle CSG is located in front of, or close to, the inferior thyroidal artery, it is an anatomic landmark for the identification of the middle CSG (17, 39-42). A typical location and direct continuity with the nerve structure are characteristic US features of the middle CSG (40).

The clinical significance of the middle CSG during the procedures could be variable depending on its location relative to the CCA. Lateral to the CCA, the middle CSG could be misinterpreted as a metastatic lymph node, possibly causing unnecessary FNA or CNB. It is vulnerable to thermal injury during RF ablation of recurrent tumors at the lateral neck. Medial to the CCA, the middle CSG closely adjacent to the thyroid gland, and could be damaged during RF ablation

Korean Journal of Radiology
KJR

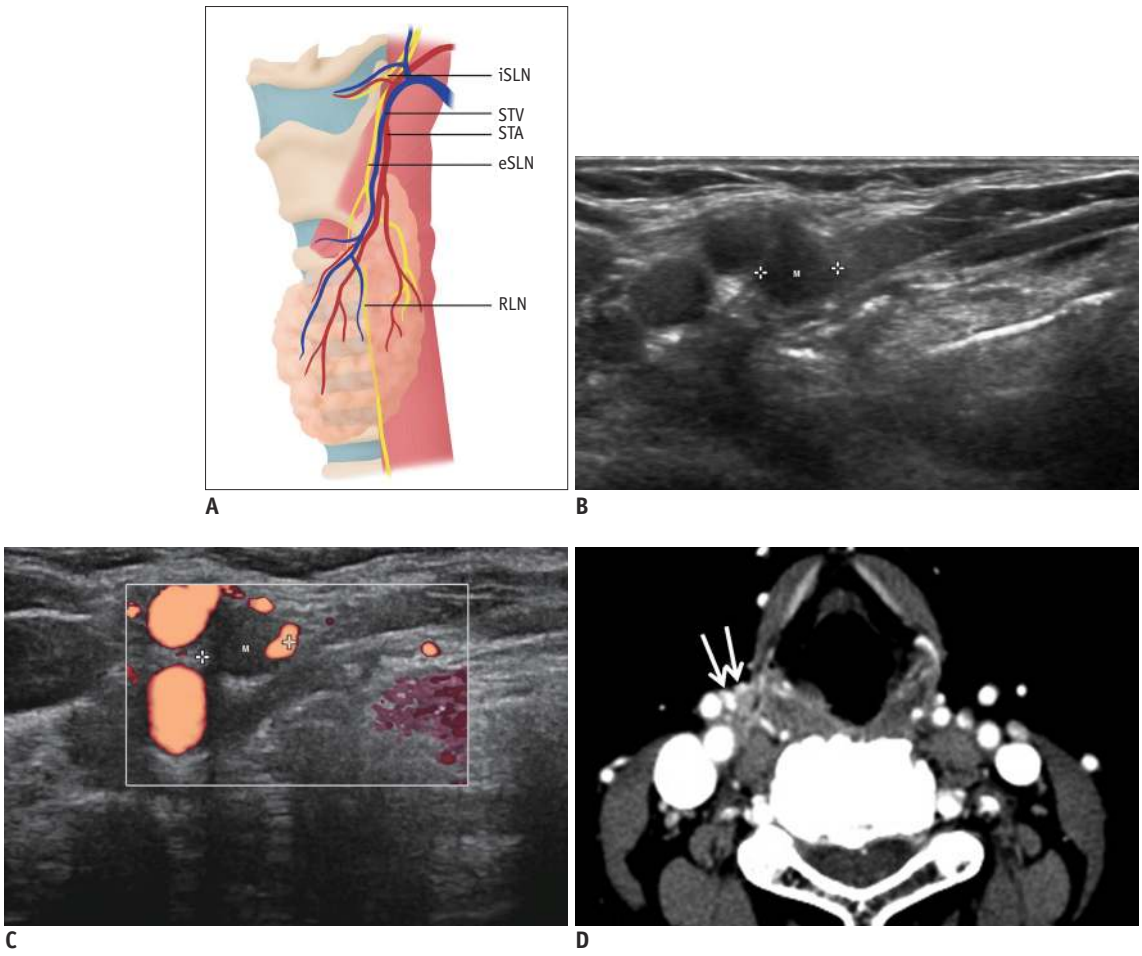

Fig. 8. Relationship of superior laryngeal nerves to adjacent anatomic structures.
A. Schematic drawing shows superior laryngeal nerve course. **B-D.** On transverse scan, metastatic lymph node (M) is seen at level of thyroid cartilage. Although superior laryngeal nerve is not directly visualized on ultrasonography, its location can be expected near superior thyroid vessels (arrows). eSLN = external branch of superior laryngeal nerve, iSLN = internal branch of superior laryngeal nerve, RLN = recurrent laryngeal nerve, STA = superior thyroid artery, STV = superior thyroid vein

near the lateral margin of benign thyroid nodules (Fig. 10) (40, 43, 44).

Injury to the CSG causes Horner syndrome, a combination of ptosis, miosis, and anhidrosis of the face on the affected side. The redness of the conjunctiva of the eye may be an initial symptom that could be used as a diagnostic sign for early detection of CSG injury (45).

Cervical Plexus and Brachial Plexus

The cervical plexus is a plexus of the ventral rami of the first 4 cervical spinal nerves, and the brachial plexus is formed by the ventral rami of the lower 4 cervical and first thoracic nerves. They are easily identified as a thin, cordlike, hypoechoic structure between the anterior and middle scalene muscles on US (4, 46-48). They first pass through the transverse process of the vertebra between the anterior and posterior tubercles, and then course between the prevertebral muscles (longus colli, longus capitis, and anterior scalene muscles) and paravertebral muscles (middle/posterior scalene, splenius cervicis, and levator scapulae muscles) deep to the sternocleidomastoid (SCM) muscle. They are subsequently located on the surface of the middle scalene and levator scapulae muscles in the posterior cervical triangle (Fig. 11) (49, 50).

Knowledge of the cervical and brachial plexus's location facilitates precise injection of the anesthetic solution for the nerve block. The cervical and brachial plexus block are used as an alternative to general anesthesia for surgery of the neck, shoulder, arm, and hand, as well as for diagnostic and therapeutic purposes for pain control (3, 16). Brachial plexus injury could occur during the RF ablation of benign thyroid nodules and recurrent thyroid cancers as well (13).

Various symptoms could be developed according to the level of cervical/brachial plexus injury. The cervical plexus

supplies the skin and muscles of the head, neck, and superior part of the shoulders; therefore, cervical plexus injury usually causes pain and paresthesia in the head and neck. The brachial plexus innervates the skin and muscles of the chest, shoulder, arm and hand, and brachial plexus injury can cause severe functional problems due to weakness of the muscles. The symptoms and signs may include a paralyzed arm, lack of muscle control in the arm, hand, or wrist, and lack of feeling or sensation.

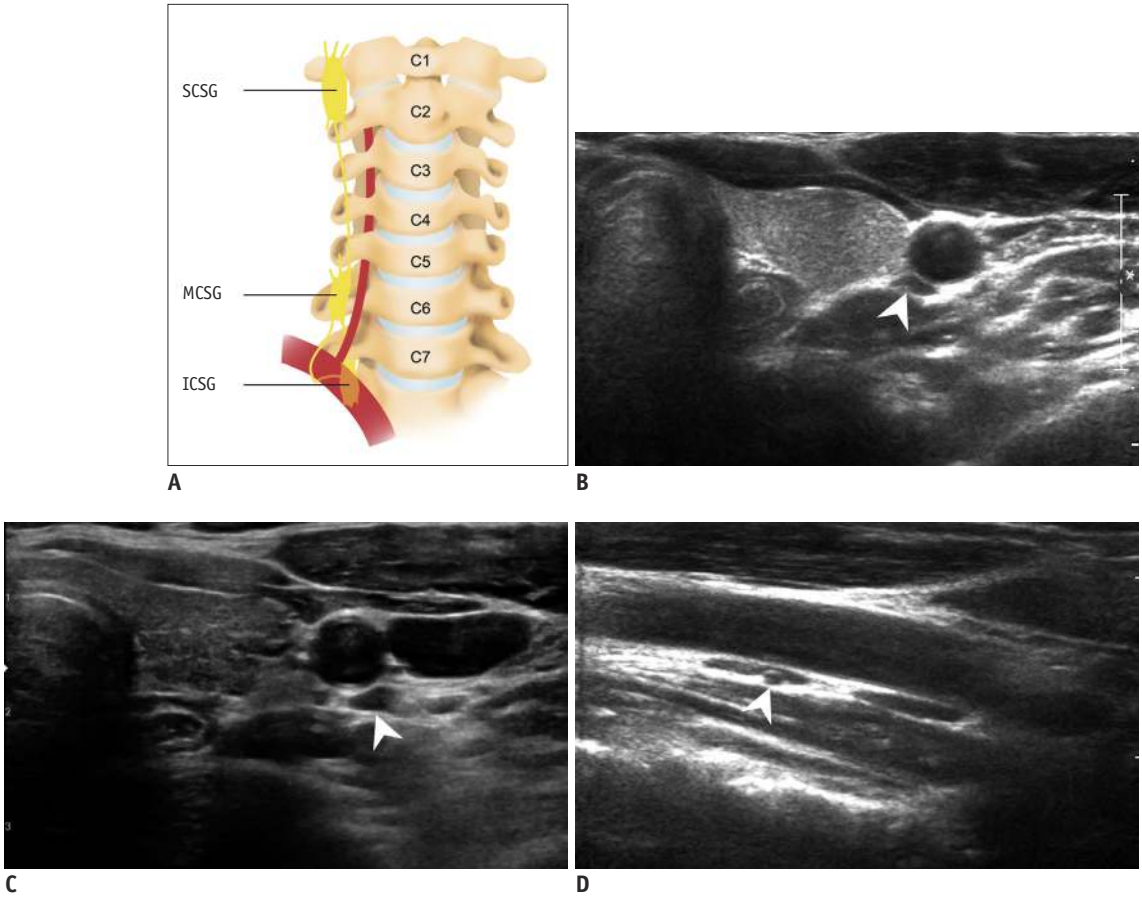

Fig. 9. Transverse ultrasonography images of MCSG.
A. Schematic drawing of cervical sympathetic ganglions. **(B, C)** MCSG (arrowheads) can be located both medially and laterally to common carotid artery, **(D)** in front of inferior thyroidal artery (arrowhead) at level of thyroid gland. ICSG = inferior cervical sympathetic ganglion, MCSG = middle cervical sympathetic ganglion, SCSG = superior cervical sympathetic ganglion

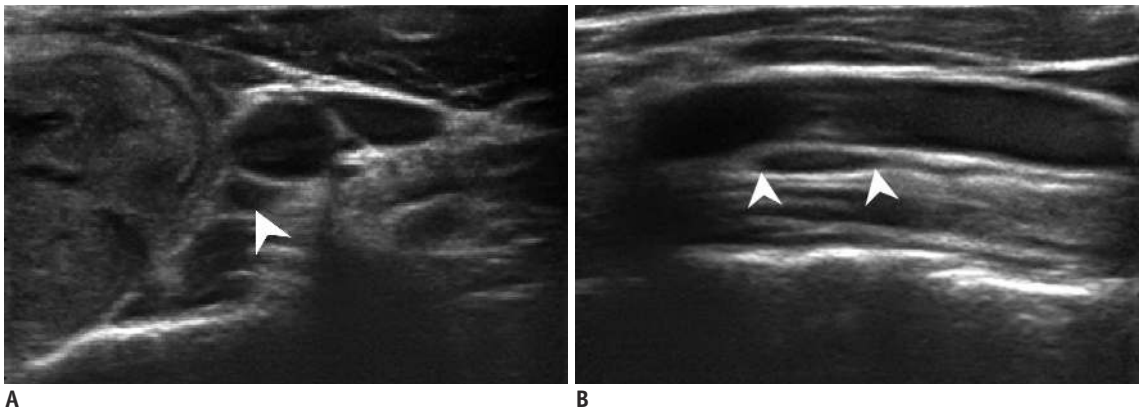

Fig. 10. Horner syndrome after RF ablation of left thyroid nodule.
On transverse **(A)** and longitudinal **(B)** ultrasonography, middle cervical sympathetic ganglion (arrowheads) are seen abutting lateral margin of ablated thyroid nodule. Horner syndrome was developed immediately after RF ablation in this patient. RF = radiofrequency

Korean Journal of Radiology
KJR

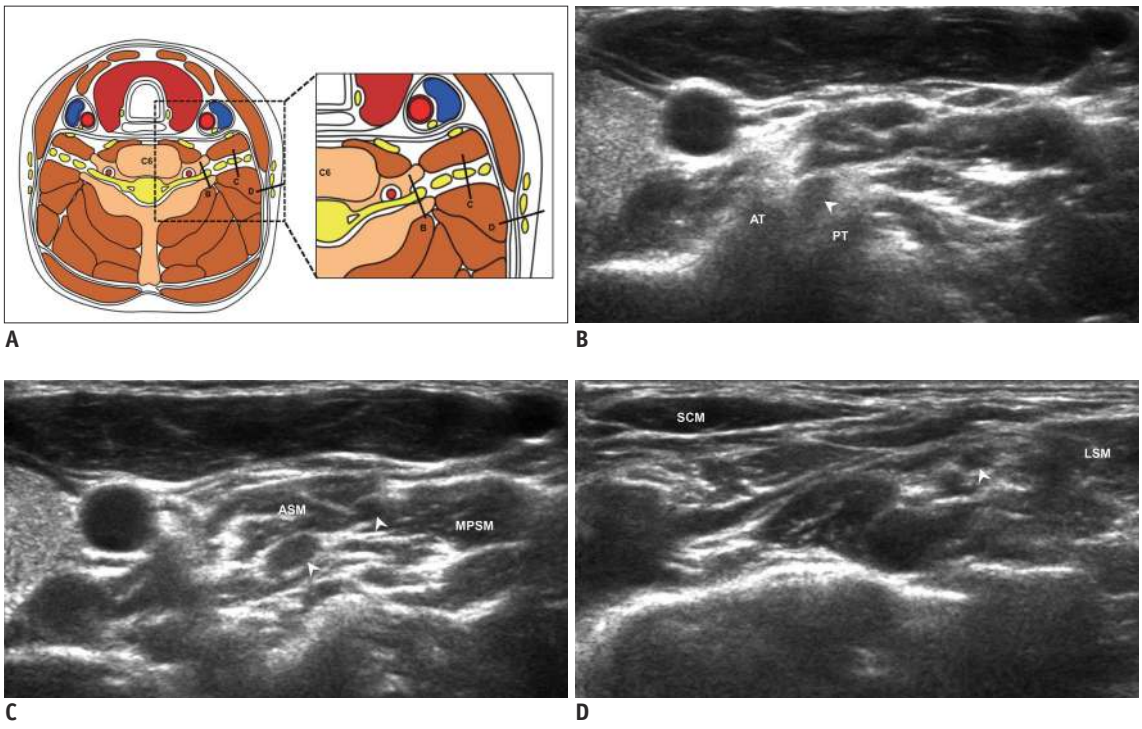

Fig. 11. Transverse ultrasonography images of cervical/brachial plexus.
A. Schematic drawing of cervical/brachial plexus course. **B.** Cervical nerve (arrowhead) passes through transverse process of vertebra between anterior and posterior tubercles. **C.** Nerve (arrowheads) courses between scalene anterior and scalene medius muscles, and **(D)** is then located in posterior cervical triangle. ASM = anterior scalene muscle, AT = anterior tubercle, LSM = levator scapulae muscle, MPSM = middle and posterior scalene muscles, PT = posterior tubercle, SCM = sternocleidomastoid muscle

Spinal Accessory Nerve

The spinal accessory nerve (SAN) is a motor nerve that supplies the SCM and trapezius muscles. The SAN can be clearly depicted between the lateroposterior border of the SCM muscle and anterior border of the trapezius muscle on US; however, it requires experience due to the thinness of the nerve (51, 52). The mean diameter of the SAN is 0.54 ± 0.09 mm (51-53), and the SAN is easily identified in the fat layer between the trapezius and levator scapulae muscles due to its superficial location. It can then be traced inferiorly into the trapezius muscle and superiorly deep into the SCM muscle, or between the 2 heads of the SCM muscle (Fig. 12) (51-54).

Due to its superficial location in the posterior cervical triangle, iatrogenic injury of the SAN is a well-known complication of surgical and minimally invasive procedures of the neck (54). Knowledge of the SAN's location on US has useful clinical applications, including optimization of surgical approaches in neck surgeries, minimization of iatrogenic SAN injuries during CNB, or RF ablation of tumors in the posterior cervical triangle. SAN dysfunction can lead to limitation of abduction of the shoulder joint, drooping of the affected shoulder, prominence of the scapula, and compensatory hypertrophy of other muscles of the affected shoulder.

Phrenic Nerve

The phrenic nerve originates from the C3–5 nerves, mainly from the C4 nerve. The phrenic nerve can be identified by US through the majority of its course. It descends obliquely anterior to the anterior scalene muscle deep, and immediately behind the SCM muscle, lateral to the IJV, and medial to the brachial plexus roots (Fig. 13). Because it crosses the transverse cervical artery along its course on the anterior scalene muscle, the transverse cervical artery is used as an anatomic landmark for detection of the phrenic nerve. The phrenic nerve crosses anterior to the first part of the subclavian artery on the left and anterior to the second part of the subclavian artery on the right (55).

Knowledge of the phrenic nerve's location may facilitate accurate injection of anesthetics in a regional nerve block and RF ablation for recurrent tumors (56, 57). Phrenic nerve injury leads to functional changes in the hemi-diaphragm, such as paralysis or hiccup. Therefore, phrenic nerve block can indeed be used for the palliative treatment of intractable hiccups related to chemotherapy and tumoral

invasion. A safer site of injection and real-time assessment of the diffusion of the anesthetic solution could minimize the side effect of phrenic nerve palsy during the brachial plexus block. Iatrogenic phrenic nerve injuries could also be prevented during CNB or RF ablation of recurrent tumors.

Traumatic Neuroma

Traumatic neuroma is caused by non-neoplastic proliferation of nerve tissue that occurs at the end of an injured nerve after trauma or surgery. It can be identified by US in 17.8% of patients after neck dissection (24). Because the traumatic neuroma usually arises from branches of the cervical plexus after neck dissection, it can be identified along the course of the cervical plexus (Fig. 14). Therefore, it is important to understand the course of the cervical plexus and its related anatomy for an accurate diagnosis of traumatic neuroma.

After neck dissection for the treatment of malignancy,

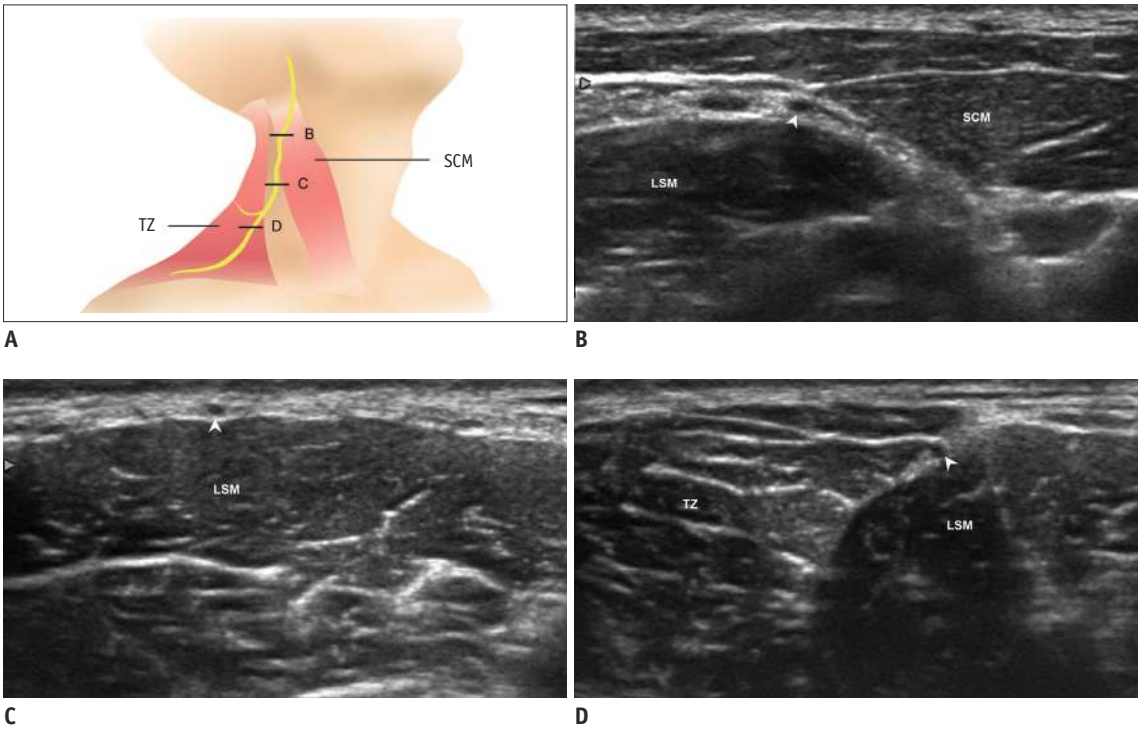

Fig. 12. Transverse ultrasonography images of SAN.
A. Schematic drawing of SAN. **B.** SAN (arrowhead) is located under SCM in upper neck. **(C)** It is located in subcutaneous layer superficial to LSM in middle (arrowhead), and **(D)** is located between TZ and LSM in lower neck (arrowhead). LSM = levator scapulae muscle, SAN = spinal accessory nerve, SCM = sternocleidomastoid muscle, TZ= trapezius muscle

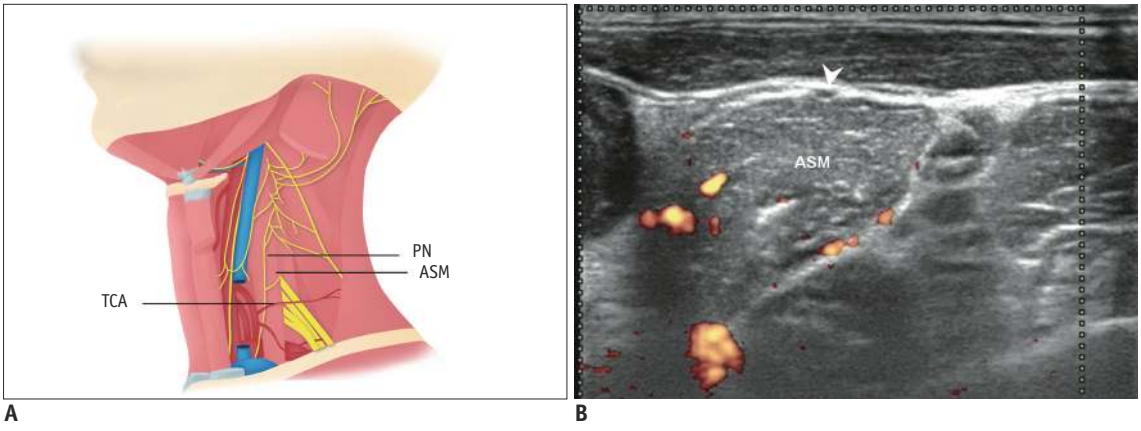

Fig. 13. Transverse ultrasonography images of phrenic nerve.
A. Schematic drawing of phrenic nerve. **B.** Phrenic nerve (arrowhead) lies superficial to ASM along its course. ASM = anterior scalene muscle, PN = phrenic nerve, TCA = transverse cervical artery

Korean Journal of Radiology
KJR

traumatic neuroma may be easily confused with a metastatic lymph node, thereby increasing patient anxiety and unnecessary FNAs. Its characteristic US feature is the direct continuity of traumatic neuroma with involved nerves at the expected position, and could lead to avoidance of unnecessary procedures. Internal linear hypoechoic structures that correspond to the neural fascicles are also very specific to traumatic neuroma (24, 58).

Muscular Structure

Muscles are the basic structures of the thyroid and neck anatomy. Knowledge of their location and relationship to small neurovascular structures is important for a safe procedure. We described the muscles that are most commonly examined in practice.

Anterior Neck Muscles

The strap muscles are a group of 4 pairs of muscles in the anterior part of the neck consisting of the thyrohyoid, sternohyoid, omohyoid, and sternothyroid muscles (Fig. 15) (59, 60). The strap muscles originate from or insert into the hyoid bone, and function to depress the hyoid bone and larynx during swallowing and speech. Because the sternothyroid and thyrohyoid muscles attach to the thyroid cartilage, the thyroid gland moves together during swallowing. The omohyoid muscle consists of superior and inferior bellies. The inferior belly forms a flat, narrow fasciculus at the lower part of the neck, and becomes tendinous behind the SCM muscle (59, 60). The tendinous portion of the omohyoid muscle can be misdiagnosed as a mass on transverse US; however, it can easily be identified by following the oblique course of the muscle on US.

The SCM muscle passes obliquely across the side of the neck, and is located anteriorly at the lower neck (Fig. 15) (59, 60). It is composed of 2 separated heads: the medial sternal head and the lateral clavicular head. Because the SCM muscle is thick and broad in shape, it is used as a primary muscular landmark of the neck and divides the neck region into anterior and posterior cervical triangles, which helps define the location of structures, such as the lymph nodes. Many neurovascular structures are closely related to the SCM muscle, including the CCA, spinal accessory nerve, and cervical/brachial plexus (46, 47, 51, 54).

Lateral Neck Muscle

The SCM muscle, scalene muscle, levator scapulae muscle, and trapezius muscle comprise the lateral part of the neck

A B C

Fig. 14. Ultrasonography (US) images of traumatic neuroma.
A. Transverse US image shows oval, heterogeneously echoic solid nodule (arrowheads) in left neck. **B, C.** Tracing of nodule in superior and medial directions shows direct continuity with cervical nerve (arrowheads) emerging from groove of transverse process. ANT = anterior, C4 = fourth cervical spine, LT = left

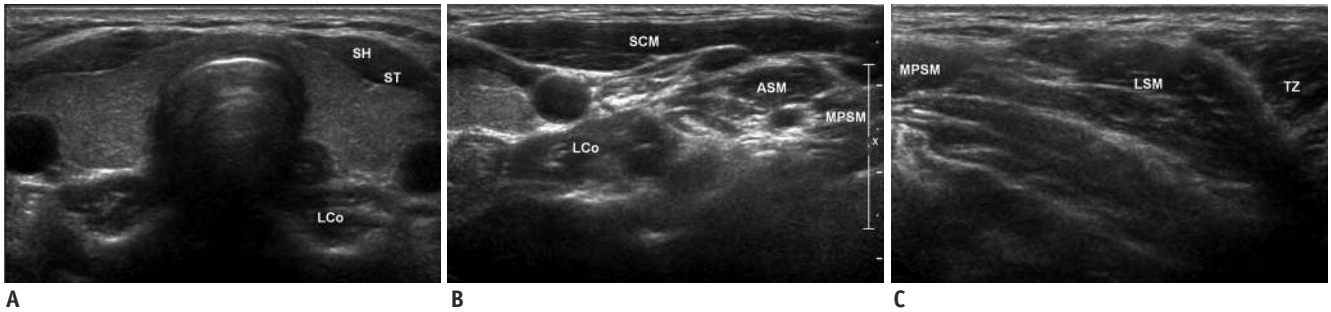

A B C

Fig. 15. Transverse ultrasonography images of neck muscles.
A-C. Muscles are basic anatomic structures for understanding thyroid and neck anatomies. ASM = anterior scalene muscle, LCo = longus colli muscle, MPSM = middle and posterior scalene muscles, SCM = sternocleidomastoid muscle, SH = sternohyoid muscle, ST = sternothyroid muscle

muscles. The scalene muscles are a group of 3 pairs of muscles in the lateral neck (anterior, middle, posterior) (Fig. 15) (59, 60). They originate from the transverse processes of the cervical vertebrae of C2 to C7, and insert into the first and second ribs. Because the cervical/brachial plexus passes between the anterior and middle scalene muscles, the scalene muscle could be an anatomical landmark for the cervical/brachial plexus, and the interscalene space is targeted with the administration of regional anesthesia for a brachial plexus block (46, 47). The phrenic nerve also passes anteriorly to the anterior scalene muscle (55).

The levator scapulae muscle originates from the dorsal tubercles of the transverse processes of C1–4, and inserts into the medial border of the scapula (59, 60). Because the SAN passes between the lateroposterior border of the SCM muscle and anterior border of the trapezius muscle, on the superficial aspect in the middle part of the levator scapulae muscle, these muscles are used as anatomical landmarks for the SAN (51, 54).

Posterior Neck Muscle

The longus colli muscle and longus capitis muscle consist of the posterior part of the neck muscles (59, 60). The longus colli muscle is in front of the spine and is the anatomical landmark for the cervical sympathetic trunk that lies on the longus colli muscle (Fig. 15) (39-42). The longus capitis muscle arises by 4 tendinous slips from the anterior tubercles of the transverse processes of C3–6. This anatomical feature easily differentiates the anterior tubercle of the transverse process from the calcified lymph node (Fig. 16).

Vascular Structure

The thyroid gland has a rich blood supply, derived from the superior, inferior, and small inferior thyroid arteries that often directly originate from the aortic arch. Venous drainage occurs via multiple surface veins draining into the superior, middle, and inferior thyroid veins (59, 60). Vascular injury could occur during the biopsy, minimally invasive treatment, or nerve block. Hematoma can be controlled by simple compression of the neck for 15–20 minutes; however, it may require surgery when complicated with abscess formation (13). We discussed the arterial and venous structures that are most commonly examined in practice.

Superior and Inferior Thyroid Artery

The superior thyroid artery arises from the external carotid artery just below the level of the greater cornu of the hyoid bone, and primarily supplies the upper and anterior part of the thyroid gland. The inferior thyroid artery arises from the thyrocervical trunk and supplies the posteroinferior parts of the gland. It is used as an anatomical landmark for the middle CSG (40). The superior thyroid artery is also used as an anatomical landmark for the external branch of the SLN (38).

Injury to the superior or inferior thyroid artery can be induced by inserting the needle or electrode at the upper and anterior part of the thyroid gland (Fig. 17). Injury to the inferior thyroid artery is more likely to result in serious problems. Because it occurs at the posteroinferior part of the thyroid gland, direct compression of the neck is less effective for bleeding control, and may cause a large amount of hematoma.

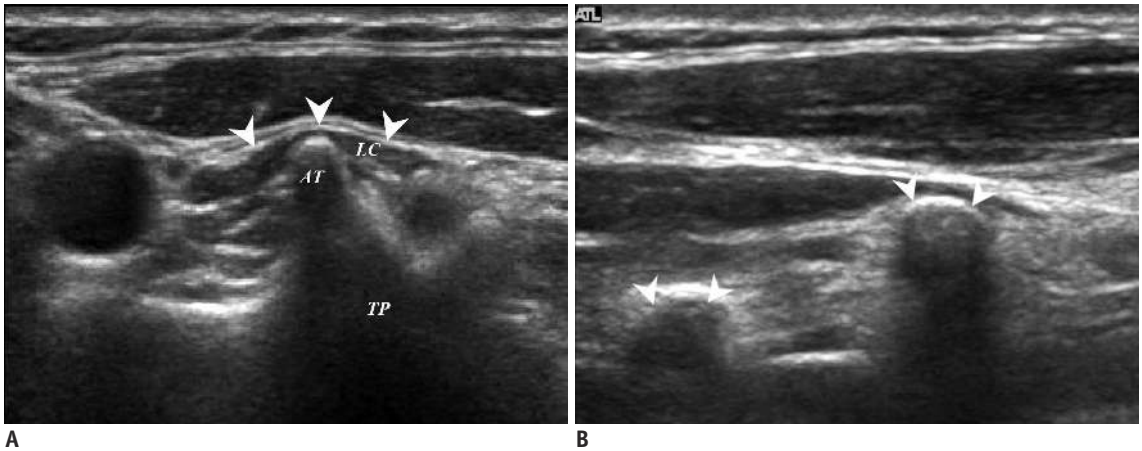

Fig. 16. Transverse and longitudinal ultrasonography images of TP.
(A) Relationship with LC (arrowheads) and **(B)** successive features on longitudinal images easily differentiate TP (arrowheads) from calcified lymph node. AT = anterior tubercle, LC = longus capitis muscle, TP = transverse process

Korean Journal of Radiology
KJR

Common Carotid Artery and Internal Jugular Vein

The CCA and IJV are typically visualized laterally adjacent to both thyroid lobes. The CCA ascends within the neck to the upper edge of the thyroid cartilage, and divides into the internal and external carotid arteries. The CCA runs behind the SCM muscle and medial to the IJV, and intersects the superior bellies of the omohyoid muscle half way up the neck (59, 60). It is necessary to measure a safe distance from the needle tip before firing the stylet for a CNB of thyroid nodules to prevent CCA injury.

The IJV originates from the jugular foramen at the base of the skull. It descends within the neck along the lateral wall of the pharynx, posterior to the internal carotid artery, and continues laterally to the CCA. It runs beneath the SCM muscle, and finally merges with the subclavian veins forming the brachiocephalic vein (59, 60).

Superior, Middle, and Inferior Thyroid Veins

The thyroid gland drains into 3 main veins, the superior, middle, and inferior thyroid veins, and each drains its respective region of the thyroid. The inferior thyroid vein arises in the venous plexus on the thyroid gland, communicating with the middle and superior thyroid veins. The superior and middle thyroid veins drain into the IJV, whereas the inferior thyroid vein drains into the brachiocephalic veins (59, 60).

Anterior Jugular Vein

The anterior jugular vein begins near the hyoid bone, and descends between the median line and anterior border of the SCM muscle. It varies considerably in size, usually inversely proportional to the external jugular vein. In most cases, there are 2 anterior jugular veins, a right and left, but occasionally only 1 vein (59, 60). It can be damaged when inserting the electrode or needle by a trans-isthmic approach in minimally invasive treatment. Because it is easily collapsed by the US probe, operators should apply soft pressure to identify the anterior jugular vein (Fig. 18). Although injury to the anterior jugular vein can be easily controlled by simple compression, it can disturb the procedure due to persistent oozing.

Fig. 17. Transverse ultrasonography images of thyroid vessels.
A. Superior thyroid artery (white arrowhead) supplies upper and anterior part of thyroid gland, and inferior thyroid artery (black arrowhead) supplies postero-inferior parts of gland. **B, C.** Pseudoaneurysm of thyroid artery (arrow) can be induced by inserting needle or electrode during procedure.

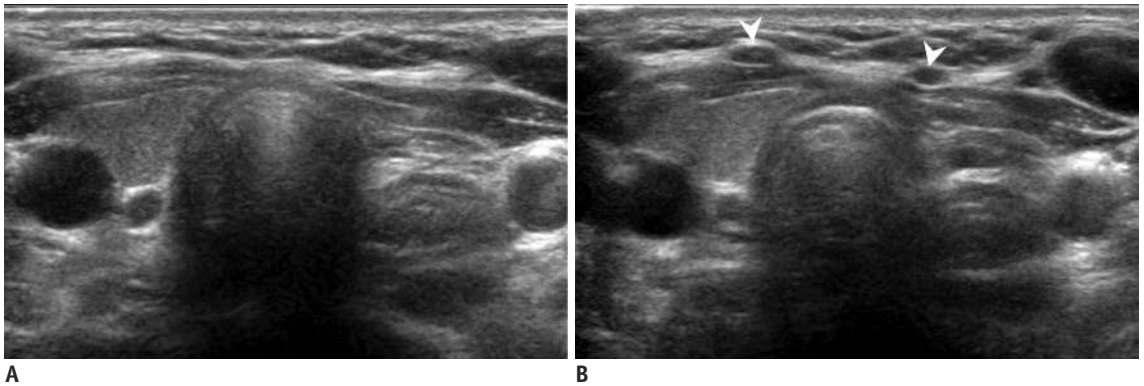

Fig. 18. Transverse ultrasonography (US) images of anterior jugular vein.
A. Anterior jugular vein can be easily collapsed by US probe, and is not visible. **B.** Therefore, operators should apply soft pressure to identify anterior jugular veins (arrowheads).

Bone and Cartilage

Bone and cartilage are the center of the thyroid and neck structures. Bony structure includes the hyoid bone and vertebrae, and appears as a bright hyperechoic linear structure with a hypoechoic acoustic shadow underneath. The cartilaginous structure includes thyroid and cricoid cartilages, and is homogeneously hypoechoic on US. However, it may be heterogeneous if it contains calcifications (Fig. 19) (61).

Hyoid Bone and Vertebrae

The hyoid bone appears as a hyperechoic inverted U-shaped linear structure with posterior acoustic shadowing on the transverse view (61). Because the thyroglossal duct cyst is located in the region of the hyoid bone, the diagnosis is based on its relationship to the hyoid bone. The pyramidal lobe is located from the isthmus toward the hyoid bone. It can persist after total thyroidectomy and is sometimes misdiagnosed as a recurred tumor.

The vertebrae are anatomical landmarks to locate the cervical and brachial plexus. Therefore, recognizing the bony structures on US images is helpful for identifying and assessing the level of the nerve roots. The absence of the anterior tubercle of the C7 transverse process and prominence of those of the C6 transverse process (Chassaignac tubercle) are used as anatomic landmarks for the identification of the cervical vertebra level (Fig. 20) (62). The transverse process of C2–5 can be identified as successive steps cranial to the C6 level. The anterior tubercle of the transverse process can be misdiagnosed as a calcified lymph node; however, it can be easily differentiated by rotating the probe and checking the successive features on longitudinal view. Vertebral injury can occur during CNB for thyroid and neck lesions, and a safe distance should be measured from the needle tip before the procedure.

Thyroid Cartilage and Cricoid Cartilage

The thyroid cartilage has an inverted V shape on the transverse view, and the true and false vocal cords are visible within the structure. The cricoid cartilage has an

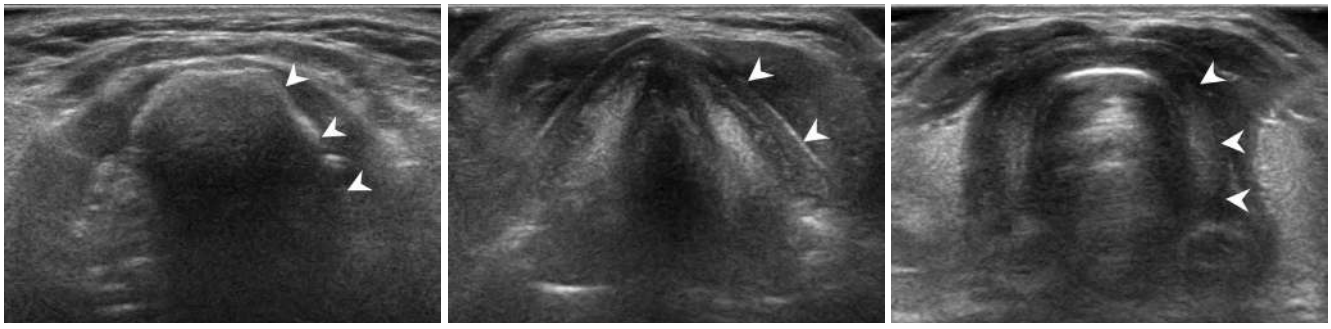

A B C

Fig. 19. Transverse ultrasonography images of bone and cartilaginous structures.
A. Hyoid bone (arrowheads) appears as hyperechoic, inverted U-shaped linear structure with posterior acoustic shadowing. **(B)** Thyroid cartilage (arrowheads) has inverted V shape, and **(C)** cricoid cartilage (arrowheads) has arch-like appearance with homogeneous hypoechogenicity.

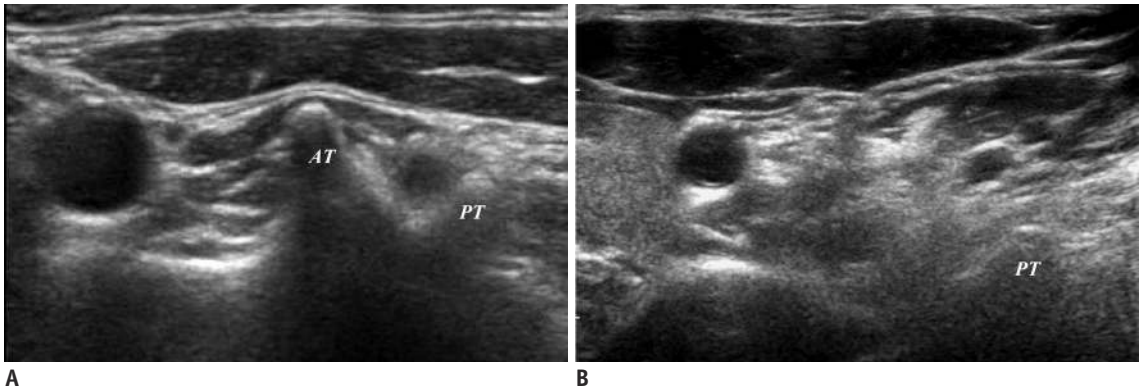

A B

Fig. 20. Transverse ultrasonography images of C6 and C7 transverse process.
A. Anterior tubercle (AT) of C6 transverse process is prominent. **B.** AT of C7 transverse process is absent. PT = posterior tubercle

Korean Journal of Radiology
KJR

arch-like appearance on the transverse view, and is located at the level of the C6 vertebra (63). The posterior surface of its anterior wall is delineated by a bright air-mucosa interface and reverberation artifacts from intraluminal air. The cricothyroid membrane and thyrohyoid membrane are seen as hyperechoic bands between the caudal and cephalad border of each cartilage. Because the SLN traverses the thyrohyoid membrane and the RLN courses close to the cricothyroid membrane, small remnants of thyroid tissue are retained after thyroid surgery to prevent nerve injury (Fig. 7).

Esophagus and Trachea

The trachea is located behind the thyroid gland, and is characterized by alternating hypo- and hyperechoic bands representing cartilaginous rings and annular ligaments on US (61). The cervical esophagus is usually seen at the left side of the trachea as a multi-layer tubular structure, which presents as an inner hyperechoic mucosa and submucosa layer, middle hypoechoic muscle layer, and an outer hyperechoic adventitial layer (46). Its location could be easily identified by asking patients to swallow, resulting in peristaltic movement of the esophagus.

The esophagus and trachea can be damaged during minimally invasive treatment such as RF ablation, although this has not yet been reported. The operators should consider the expected ablation zone and strictly trace the tip of the electrode during the ablation of nodules near the esophagus or trachea.

Prevention Techniques

Careful US examination, along with knowledge of US-based thyroid and neck anatomy, is necessary to prevent

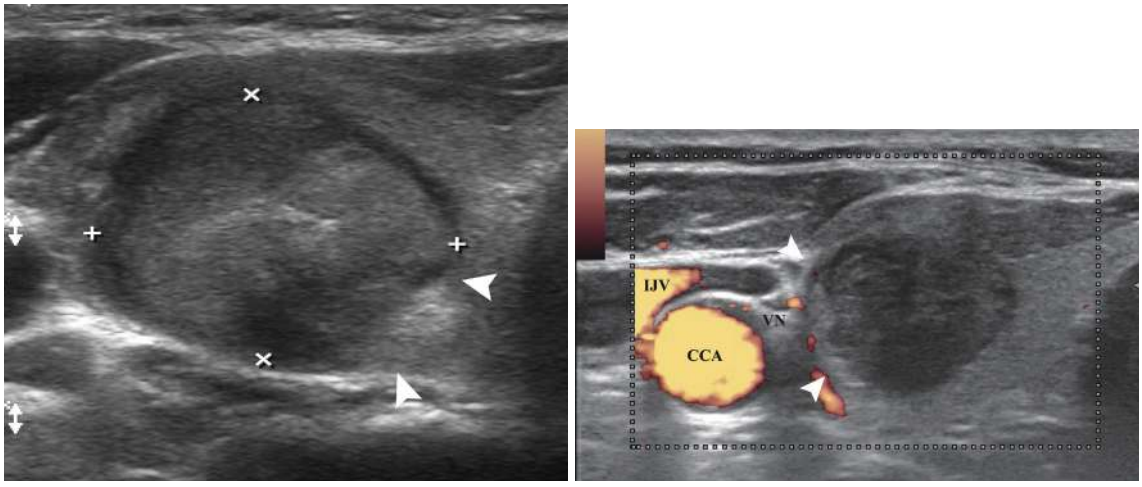

A B

Fig. 21. Undertreatment of nodule margin to prevent nerve injury.
A. On transverse scan, recurrent laryngeal nerve injury could be prevented by undertreating nodule near danger triangle (arrowheads). **B.** Operators should be familiar with antomical variation in vagus nerve (VN), which is located adjacent to thyroid gland (arrowheads) to prevent nerve injury. CCA = common carotid artery, IJV = internal jugular vein

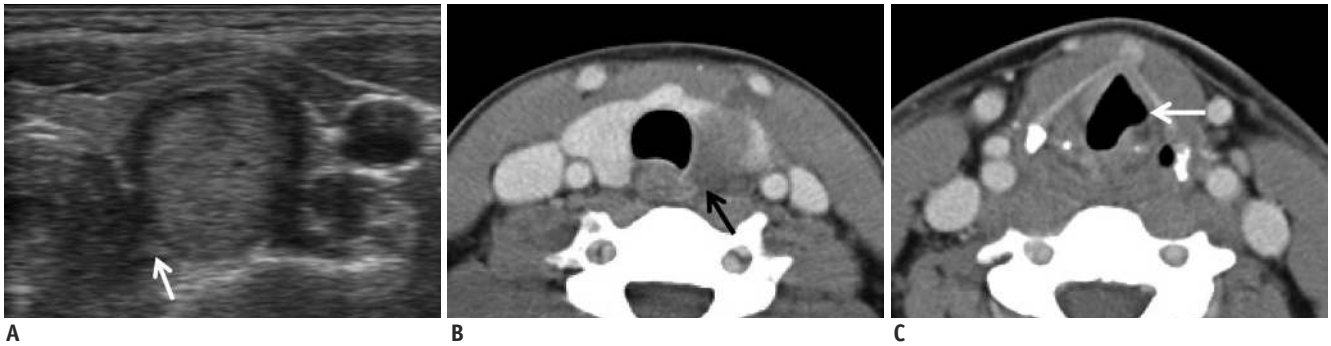

A B C

Fig. 22. Vocal cord paralysis after radiofrequency ablation of left thyroid nodule.
Transverse ultrasonography **(A)** and CT **(B)** image show large ablated zone including tracheoesophageal groove (arrows). **C.** Vocal cord paralysis was confirmed on CT image (arrow).

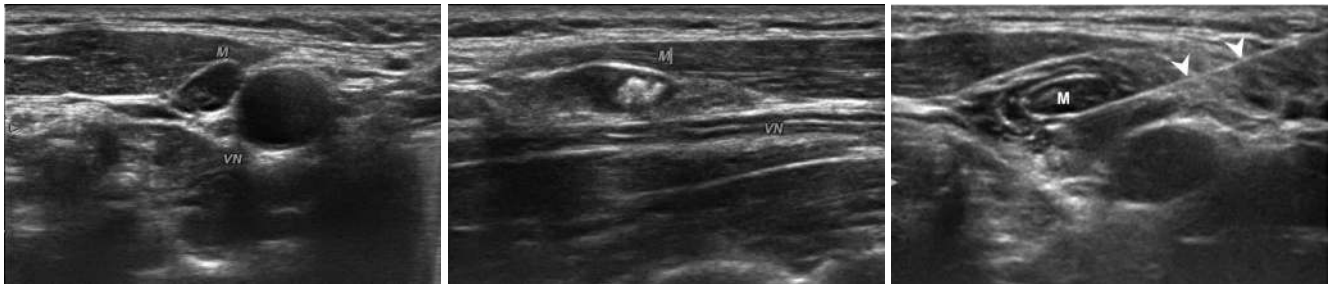

A B C

Fig. 23. Hydrodissection technique.
A, B. On transverse and longitudinal images, VN is located adjacent to metastatic tumor. **C.** 5% dextrose solution is carefully injected between nerve and tumor to prevent needle-induced thermal injury (arrowheads). M = mass, VN = vagus nerve

complications during the US-guided procedures. Nerves of the neck should be thoroughly evaluated for minimally invasive treatment of benign and recurrent thyroid tumors. The danger triangle could remain undertreated because of its close approximation to the RLN, trachea, or esophagus. Any expected location of nerve injuries, particularly for the vagus nerve and middle CSG, could be undertreated (Figs. 21, 22). If a metastatic tumor is adjacent to the nerve, the hydrodissection technique involving injection of a 5% dextrose solution between the nerve and tumor, could be useful for preventing thermal injury (Fig. 23).

Serious hemorrhage could be prevented by examining the perithyroidal vessels before the procedure. The needle should be advanced carefully within the nodule or across the nodule's margin to obtain a tissue core for the thyroid, but the needle tip should not be moved ahead across the thyroid capsule to prevent ITA injury. When using the automated gun, a safe distance should be measured from the needle tip before firing the stylet. Intranodular hemorrhage caused by an RF electrode can be controlled using direct ablation of the hemorrhagic focus.

Esophageal injury may be prevented by maintaining a safety margin between the esophagus and tip of the RF electrode. Swallowing cold water during the procedure can decrease the temperature of the esophagus, and increased esophageal peristalsis can also prevent thermal injury to the esophagus. Coughing could be induced by thermal propagation to the trachea. The procedure should be stopped immediately when coughing is induced and any possible heat injury to the trachea should be evaluated.

CONCLUSION

Knowledge of US-based thyroidal and perithyroidal anatomy, its clinical significance, and prevention techniques may help in the early detection, prevention, and proper management of complications during US-guided procedures.

REFERENCES

1. Gharib H, Hegedüs L, Pacella CM, Baek JH, Papini E. Clinical review: nonsurgical, image-guided, minimally invasive therapy for thyroid nodules. *J Clin Endocrinol Metab* 2013;98:3949-3957
2. Na DG, Lee JH, Jung SL, Kim JH, Sung JY, Shin JH, et al. Radiofrequency ablation of benign thyroid nodules and recurrent thyroid cancers: consensus statement and recommendations. *Korean J Radiol* 2012;13:117-125
3. Kapral S, Greher M, Huber G, Willschke H, Kettner S, Kdolsky R, et al. Ultrasonographic guidance improves the success rate of interscalene brachial plexus blockade. *Reg Anesth Pain Med* 2008;33:253-258
4. Soeding P, Eizenberg N. Review article: anatomical considerations for ultrasound guidance for regional anesthesia of the neck and upper limb. *Can J Anaesth* 2009;56:518-533
5. Yeon JS, Baek JH, Lim HK, Ha EJ, Kim JK, Song DE, et al. Thyroid nodules with initially nondiagnostic cytologic results: the role of core-needle biopsy. *Radiology* 2013;268:274-280
6. Na DG, Kim JH, Sung JY, Baek JH, Jung KC, Lee H, et al. Core-needle biopsy is more useful than repeat fine-needle aspiration in thyroid nodules read as nondiagnostic or atypia of undetermined significance by the Bethesda system for reporting thyroid cytopathology. *Thyroid* 2012;22:468-475
7. Lee SH, Kim MH, Bae JS, Lim DJ, Jung SL, Jung CK. Clinical outcomes in patients with non-diagnostic thyroid fine needle aspiration cytology: usefulness of the thyroid core needle biopsy. *Ann Surg Oncol* 2014;21:1870-1877
8. Trimboli P, Nasrollah N, Guidobaldi L, Taccogna S, Cicciarella Modica DD, Amendola S, et al. The use of core needle biopsy as first-line in diagnosis of thyroid nodules reduces false negative and inconclusive data reported by fine-needle aspiration. *World J Surg Oncol* 2014;12:61
9. Ha EJ, Baek JH, Lee JH, Kim JK, Kim JK, Lim HK, et al. Core needle biopsy can minimise the non-diagnostic results and need for diagnostic surgery in patients with calcified thyroid nodules. *Eur Radiol* 2014;24:1403-1409
10. Ha EJ, Baek JH, Lee JH, Song DE, Kim JK, Shong YK, et al.

Sonographically suspicious thyroid nodules with initially benign cytologic results: the role of a core needle biopsy. *Thyroid* 2013;23:703-708
11. Kim BM, Kim EK, Kim MJ, Yang WI, Park CS, Park SI. Sonographically guided core needle biopsy of cervical lymphadenopathy in patients without known malignancy. *J Ultrasound Med* 2007;26:585-591
12. Screaton NJ, Berman LH, Grant JW. Head and neck lymphadenopathy: evaluation with US-guided cutting-needle biopsy. *Radiology* 2002;224:75-81
13. Baek JH, Lee JH, Sung JY, Bae JI, Kim KT, Sim J, et al. Complications encountered in the treatment of benign thyroid nodules with US-guided radiofrequency ablation: a multicenter study. *Radiology* 2012;262:335-342
14. Kaufman MR, Elkwood AI, Rose MI, Patel T, Ashinoff R, Fields R, et al. Surgical treatment of permanent diaphragm paralysis after interscalene nerve block for shoulder surgery. *Anesthesiology* 2013;119:484-487
15. Jeng CL, Torrillo TM, Rosenblatt MA. Complications of peripheral nerve blocks. *Br J Anaesth* 2010;105 Suppl 1:i97-i107
16. Usui Y, Kobayashi T, Kakinuma H, Watanabe K, Kitajima T, Matsuno K. An anatomical basis for blocking of the deep cervical plexus and cervical sympathetic tract using an ultrasound-guided technique. *Anesth Analg* 2010;110:964-968
17. Bhatia A, Flamer D, Peng PW. Evaluation of sonoanatomy relevant to performing stellate ganglion blocks using anterior and lateral simulated approaches: an observational study. *Can J Anaesth* 2012;59:1040-1047
18. Chiou HJ, Chou YH, Chiou SY, Liu JB, Chang CY. Peripheral nerve lesions: role of high-resolution US. *Radiographics* 2003;23:e15
19. Fornage BD. Peripheral nerves of the extremities: imaging with US. *Radiology* 1988;167:179-182
20. Giovagnorio F, Martinoli C. Sonography of the cervical vagus nerve: normal appearance and abnormal findings. *AJR Am J Roentgenol* 2001;176:745-749
21. Knappertz VA, Tegeler CH, Hardin SJ, McKinney WM. Vagus nerve imaging with ultrasound: anatomic and in vivo validation. *Otolaryngol Head Neck Surg* 1998;118:82-85
22. Donatini G, Iacconi P, De Bartolomeis C, Iacconi C, Fattori S, Pucci A, et al. Neck lesions mimicking thyroid pathology. *Langenbecks Arch Surg* 2009;394:435-440
23. Ha EJ, Baek JH, Lee JH, Kim JK, Shong YK. Clinical significance of vagus nerve variation in radiofrequency ablation of thyroid nodules. *Eur Radiol* 2011;21:2151-2157
24. Ha EJ, Baek JH, Lee JH, Kim YJ, Kim JK, Kim TY, et al. Characteristic ultrasound feature of traumatic neuromas after neck dissection: direct continuity with the cervical plexus. *Thyroid* 2012;22:820-826
25. Park JK, Jeong SY, Lee JH, Lim GC, Chang JW. Variations in the course of the cervical vagus nerve on thyroid ultrasonography. *AJNR Am J Neuroradiol* 2011;32:1178-1181
26. Le Corroller T, Sebag F, Vidal V, Jacquier A, Champsaur P, Bartoli JM, et al. Sonographic diagnosis of a cervical vagal schwannoma. *J Clin Ultrasound* 2009;37:57-60
27. Mra Z, Wax MK. Nonrecurrent laryngeal nerves: anatomic considerations during thyroid and parathyroid surgery. *Am J Otolaryngol* 1999;20:91-95
28. Henry JF, Audiffret J, Denizot A, Plan M. The nonrecurrent inferior laryngeal nerve: review of 33 cases, including two on the left side. *Surgery* 1988;104:977-984
29. Gray SW, Skandalakis JE, Akin JT Jr. Embryological considerations of thyroid surgery: developmental anatomy of the thyroid, parathyroids and the recurrent laryngeal nerve. *Am Surg* 1976;42:621-628
30. Avisse C, Marcus C, Delattre JF, Marcus C, Cailliez-Tomasi JP, Palot JP, et al. Right nonrecurrent inferior laryngeal nerve and arteria lusoria: the diagnostic and therapeutic implications of an anatomic anomaly. Review of 17 cases. *Surg Radiol Anat* 1998;20:227-232
31. Gong RX, Luo SH, Gong YP, Wei T, Li ZH, Huang JB, et al. Prediction of nonrecurrent laryngeal nerve before thyroid surgery--experience with 1825 cases. *J Surg Res* 2014;189:75-80
32. Yetisir F, Salman AE, Çiftçi B, Teber A, Kiliç M. Efficacy of ultrasonography in identification of non-recurrent laryngeal nerve. *Int J Surg* 2012;10:506-509
33. Huang SM, Wu TJ. Neck ultrasound for prediction of right nonrecurrent laryngeal nerve. *Head Neck* 2010;32:844-849
34. Tomoda C, Takamura Y, Ito Y, Miya A, Miyauchi A. Transient vocal cord paralysis after fine-needle aspiration biopsy of thyroid tumor. *Thyroid* 2006;16:697-699
35. Shin JE, Baek JH, Lee JH. Radiofrequency and ethanol ablation for the treatment of recurrent thyroid cancers: current status and challenges. *Curr Opin Oncol* 2013;25:14-19
36. Shin JH, Baek JH, Ha EJ, Lee JH. Radiofrequency ablation of thyroid nodules: basic principles and clinical application. *Int J Endocrinol* 2012;2012:919650
37. Sasou S, Nakamura S, Kurihara H. Suspensory ligament of Berry: its relationship to recurrent laryngeal nerve and anatomic examination of 24 autopsies. *Head Neck* 1998;20:695-698
38. Barberet G, Henry Y, Tatu L, Berthier F, Besch G, Pili-Floury S, et al. Ultrasound description of a superior laryngeal nerve space as an anatomical basis for echoguided regional anaesthesia. *Br J Anaesth* 2012;109:126-128
39. Saylam CY, Ozgiray E, Orhan M, Cagli S, Zileli M. Neuroanatomy of cervical sympathetic trunk: a cadaveric study. *Clin Anat* 2009;22:324-330
40. Shin JE, Baek JH, Ha EJ, Choi YJ, Choi WJ, Lee JH. Ultrasound features of middle cervical sympathetic ganglion. *Clin J Pain* 2014 Nov 19 [Epub ahead of print]
41. Kiray A, Arman C, Naderi S, Güvencer M, Korman E. Surgical anatomy of the cervical sympathetic trunk. *Clin Anat* 2005;18:179-185
42. Gofeld M, Bhatia A, Abbas S, Ganapathy S, Johnson M. Development and validation of a new technique for ultrasound-guided stellate ganglion block. *Reg Anesth Pain Med* 2009;34:475-479

43. Pishdad GR, Pishdad P, Pishdad R. Horner's syndrome as a complication of percutaneous ethanol treatment of thyroid nodule. *Thyroid* 2011;21:327-328
44. Messika O, Telman G. Horner syndrome after lymph node fine needle aspiration. *Acta Cytol* 2009;53:487-488
45. Lee JH, Lee HK, Lee DH, Choi CG, Kim SJ, Suh DC. Neuroimaging strategies for three types of Horner syndrome with emphasis on anatomic location. *AJR Am J Roentgenol* 2007;188:W74-W81
46. Gervasio A, Mujahed I, Biasio A, Alessi S. Ultrasound anatomy of the neck: the infrahyoid region. *J Ultrasound* 2010;13:85-89
47. Ihnatsenka B, Boezaart AP. Applied sonoanatomy of the posterior triangle of the neck. *Int J Shoulder Surg* 2010;4:63-74
48. Roessel T, Wiessner D, Heller AR, Zimmermann T, Koch T, Litz RJ. High-resolution ultrasound-guided high interscalene plexus block for carotid endarterectomy. *Reg Anesth Pain Med* 2007;32:247-253
49. Narouze S. Sonoanatomy of the cervical spinal nerve roots: implications for brachial plexus block. *Reg Anesth Pain Med* 2009;34:616
50. Demondion X, Herbinet P, Boutry N, Fontaine C, Francke JP, Cotten A. Sonographic mapping of the normal brachial plexus. *AJNR Am J Neuroradiol* 2003;24:1303-1309
51. Canella C, Demondion X, Abreu E, Marchiori E, Cotten H, Cotten A. Anatomical study of spinal accessory nerve using ultrasonography. *Eur J Radiol* 2013;82:56-61
52. Mirjalili SA, Muirhead JC, Stringer MD. Ultrasound visualization of the spinal accessory nerve in vivo. *J Surg Res* 2012;175:e11-e16
53. Seok JI, Kim JW, Walker FO. Spontaneous spinal accessory nerve palsy: the diagnostic usefulness of ultrasound. *Muscle Nerve* 2014;50:149-150
54. Hong MJ, Baek JH, Kim DY, Ha EJ, Choi WJ, Choi YJ, et al. Spinal accessory nerve: ultrasound findings and correlations with neck lymph node levels. *Ultraschall Med* 2014 Dec 17 [Epub ahead of print]
55. Canella C, Demondion X, Delebarre A, Moraux A, Cotten H, Cotten A. Anatomical study of phrenic nerve using ultrasound. *Eur Radiol* 2010;20:659-665
56. Kuusniemi K, Pyylampi V. Phrenic nerve block with ultrasound-guidance for treatment of hiccups: a case report. *J Med Case Rep* 2011;5:493
57. Kang KN, Park IK, Suh JH, Leem JG, Shin JW. Ultrasound-guided Pulsed Radiofrequency Lesioning of the Phrenic Nerve in a Patient with Intractable Hiccup. *Korean J Pain* 2010;23:198-201
58. Ha EJ, Lee JH, Lim HK, Bae Kim W, Baek JH. Identification of continuity of transected nerve on sonography after neck dissection: direct sign of traumatic neuroma. *Thyroid* 2011;21:1385-1387
59. Standring S. *Gray's Anatomy: The Anatomical Basis of Clinical Practice, Expert Consult*. London: Churchill Livingstone, 2008
60. Jacob S. *Human anatomy: A Clinically-Orientated Approach*. New York: Elsevier, 2008
61. Singh M, Chin KJ, Chan VW, Wong DT, Prasad GA, Yu E. Use of sonography for airway assessment: an observational study. *J Ultrasound Med* 2010;29:79-85
62. van Eerd M, Patijn J, Sieben JM, Sommer M, Van Zundert J, van Kleef M, et al. Ultrasonography of the cervical spine: an in vitro anatomical validation model. *Anesthesiology* 2014;120:86-96
63. Strauss S. Cricoid cartilage masquerading as a tumour on thyroid ultrasound. *Br J Radiol* 1999;72:644-647